OXFORD

Research Article

Analysis of cysteine-X-cysteine motif chemokine ligands 9, 10, and 11, their receptor CXCR3, and their possible role on the recruitment of immune cells at the maternal–conceptus interface in pigs[†]

Jisoo Han[1], Min Jeong Gu[2], Inkyu Yoo[1], Yohan Choi[1], Hwanhee Jang[1], Minjeong Kim[1], Cheol-Heui Yun[2] and Hakhyun Ka[1,*]

[1]Department of Biological Science and Technology, Yonsei University, Wonju, Republic of Korea and [2]Department of Agricultural Biotechnology, Research Institute for Agriculture and Life Sciences, Seoul National University, Seoul, Republic of Korea

*Correspondence: Department of Biological Science and Technology, Yonsei University, Wonju 220-710, Republic of Korea. Tel: +82-33-760-2369; Fax: +82-33-760-2183; E-mail: hka@yonsei.ac.kr

Abstract

Chemokines play critical roles in the establishment and maintenance of pregnancy in animals. Cysteine-X-cysteine motif chemokine ligand 9 (CXCL9), CXCL10, and CXCL11 are involved in recruiting immune cells by binding to their shared receptor, CXC receptor 3 (CXCR3), in a variety of tissues. This study examined the expression and regulation of chemokines *CXCL9*, *CXCL10*, and *CXCL11*, their receptor *CXCR3*, and their role at the maternal–conceptus interface in pigs. The endometrium expressed *CXCL9*, *CXCL10*, *CXCL11*, and *CXCR3* stage specifically during pregnancy, with the greatest abundance on Day 15 of pregnancy. It was noted that their expression was primarily localized to stromal cells, endothelial cells, or vascular smooth muscle cells in the endometrium. Interferon-γ increased the abundance of *CXCL9*, *CXCL10*, *CXCL11* mRNAs, but not *CXCR3*, in endometrial explants. Furthermore, recombinant CXCL9 (rCXCL9), rCXCL10, and rCXCL11 proteins increased migration of cultured peripheral blood mononuclear cells (PBMCs) in a dose-dependent manner. Recombinant CXCL9 and rCXCL10 caused migration of CD4$^+$, CD8$^+$, CD4$^+$CD8$^+$ T cells, and natural killer (NK) cells, and rCXCL11 increased migration of CD4$^+$ T and NK cells in PBMCs. The present study demonstrated that interferon-γ-induced *CXCL9*, *CXCL10*, and *CXCL11*, and their receptor *CXCR3* were expressed in the uterus in stage- and cell-type specific manners and increased the migration of T and NK cells, which showed the greatest endometrial infiltration on Day 15 of pregnancy. These results suggest that CXCL9, CXCL10, and CXCL11 may play an important role in the recruitment of immune cells into the endometrium during the implantation period in pigs.

Summary Sentence

Chemokines CXCL9, 10, and 11 induced by interferon-gamma of conceptus origin in the endometrium are involved in the recruitment of immune cells at the maternal-conceptus interface in pigs.

Key words: pig, pregnancy, uterus, endometrium, CXCL9, CXCL10, CXCL11.

Introduction

The establishment and maintenance of pregnancy require appropriate interactions between the developing conceptus (embryo/fetus and associated extraembryonic membranes) and the maternal endometrium. During the peri-implantation period in pigs, the conceptuses elongate from 5 mm to almost 1 m in length and change morphology from spherical to tubular and to filamentous forms [1]. In addition, the conceptuses secrete estrogen that functions as the maternal recognition signal of pregnancy to redirect prostaglandin $F_{2\alpha}$ ($PGF_{2\alpha}$) secretion from the uterine vasculature to the uterine lumen for corpora lutea maintenance [1]. Elongating conceptuses also produce interleukin-1β2(IL1B2) into the uterine lumen [1, 2], which acts to induce the expression of IL1 receptor 1 (*IL1R1*), IL1 receptor accessory protein (*IL1RAP*), and the PG-synthetic enzymes *AKR1B1* (aldo-keto reductase family 1, member B1), *PTGS1* (prostaglandin-endoperoxide synthase 1), and *PTGS2* (prostaglandin-endoperoxide synthase 2), and the PG transporters *ABCC4* (ATP-binding cassette subfamily C member 4) and *SLCO2A1* (solute carrier organic anion transporter family, member 2A1) in the endometrium [3–5]. Subsequently, the elongated porcine conceptuses intensively produce two types of interferons (IFNs), IFN-δ (IFND, a type I IFN) and IFN-γ (IFNG, a type II IFN), during the peri-implantation period [6].

IFNs are a group of cytokines that have antiviral, antiproliferative, and immunomodulatory effects in vertebrates [7]. In ruminants, it is well known that IFN-τ (IFNT), a type I IFN produced by the implanting conceptus, acts as a maternal recognition of the pregnancy signal by suppressing endometrial expression of estrogen receptor (*ESR1*) and oxytocin receptor (*OXTR*) to block production of $PGF_{2\alpha}$, resulting in the maintenance of ovarian progesterone production [8]. In pigs, however, the conceptus-derived IFNs do not have an antiluteolytic effect [9, 10]. Rather, it has been suggested that they regulate trophoblast attachment [6, 9] and increase PGE_2 secretion and endometrial gene expression related to maternal immune reactions, including major histocompatibility complex class I, β2-microglobulin, signal transducer and activator of transcription 1 (STAT1), and interferon regulatory factor 1 (IRF1) [11, 12]. Nevertheless, the precise mechanisms of action of conceptus-derived IFND and IFNG are not fully understood in pigs.

Chemokines constitute a family of closely related chemoattractant cytokines that promote the recruitment and activation of various immune cells [13]. The chemokines are classified into cysteine (C), cysteine-cysteine (C-C), cysteine-X-cysteine (C-X-C), and cysteine-X-3 cysteines (C-X-3C) subsets based on the conserved cysteine motifs [14]. Cysteine-X-cysteine chemokine ligand 9 (CXCL9; also called monokine induced by gamma interferon, MIG), CXCL10 (also called interferon gamma-induced protein 10, IP-10), and CXCL11 (also called interferon-gamma-inducible protein 9, IP-9 and interferon-inducible T-cell alpha chemoattractant, I-TAC) have been identified as the CXC chemokines that are induced by IFNG and secreted by various cell types, including endothelial cells, lymphocytes, and hematopoietic progenitor cells [15–18]. They are small proteins that bind to a shared G protein-coupled receptor, CXC chemokine receptor 3 (CXCR3) [16, 17]. CXCR3 is expressed by various immune cells, including CD4$^+$ and CD8$^+$ T cells, natural killer (NK) cells, NKT cells, a subset of B cells, monocytes, dendritic cells, and nonimmune cells such as endothelial cells and neurons [19, 20]. CXCL9, CXCL10, and CXCL11 are known to regulate immune responses by recruitment and activation of CXCR3-expressing leukocytes into inflamed tissues and play important roles in the pathophysiology of autoimmune diseases and viral infections [17, 21–23].

Production of CXCL9, CXCL10, and CXCL11, and their receptor CXCR3 by the endometrium has been reported in some species. In humans, CXCL9, CXCL10, and CXCL11 are expressed in endometrial epithelial cells and stromal cells, while CXCR3 is expressed on endometrial epithelial, stromal, trophoblast, and NK cells, indicating that these chemokines act in autocrine and paracrine fashions and recruit NK cells into the uterus [24–26]. CXCL9, CXCL10, and CXCL11 are also expressed in the ovine endometrium at the time of conceptus implantation, and their expression is increased by IFNT and IFNG in endometrial explants [27, 28]. Ovine trophoblast cells express CXCR3, and CXCL9 and CXCL10 increase attachment of trophoblast cells to endometrial epithelial cells [28]. In addition, it has been reported in goats that CXCL10 is expressed in the endometrial stroma, and CXCR3 is expressed in the implanting conceptus and immune cells, indicating that CXCL10 induces migration and adhesion of trophoblast cells and recruitment of immune cells into the endometrium [29, 30]. Still, very little is known about the expression and function of CXCL9, CXCL10, and CXCL11, and their receptor CXCR3 in the endometrium in pigs.

To test the hypothesis that CXCL9, CXCL10, and CXCL11 are produced by endometrial cells in response to IFNG of conceptus origin and act on recruitment of immune cells from circulating blood into the endometrial tissues in pigs, this study determined: (1) the expression of *CXCL9*, *CXCL10*, *CXCL11*, and *CXCR3* in the endometrium during the estrous cycle and pregnancy and in conceptuses during early pregnancy and chorioallantoic tissues during mid- to late pregnancy; (2) the localization of *CXCL9*, *CXCL10*, *CXCL11*, and *CXCR3* at the maternal–conceptus interface; (3) the effect of IFNG on *CXCL9*, *CXCL10*, *CXCL11*, and *CXCR3* expression in endometrial tissues; (4) the effect of CXCL9, CXCL10, and CXCL11 on migration of peripheral blood mononuclear cells (PBMCs); and (5) the infiltration of T cells and NK cells into the endometrium during the estrous cycle and pregnancy.

Materials and methods

Animals and tissue preparation

All experimental procedures involving animals were conducted in accordance with the Guide for Care and Use of Research Animals in Teaching and Research and were approved by the Institutional Animal Care and Use Committee of Yonsei University and Seoul National University. Sexually mature crossbred female pigs were assigned randomly to either cyclic or pregnant status. The reproductive tracts of gilts were obtained immediately after slaughter on either Day 12 or 15 of the estrous cycle or Day 12, 15, 30, 60, 90, or 114 of pregnancy (n = 4–6 gilts/day/status). Pregnancy was confirmed by

Table 1. Summary of PCR primer sequences and expected product sizes.

Primer	Sequence of forward (F) and reverse (R) primers (5′ → 3′)	Annealing temperature (°C)	Product size (bp)	No. of cycles	GenBank accession no.
For real-time RT-PCR					
CXCL9	F: GTA TCA TCT TCC TGA CTC TGA TTG G	60	276	40	NM 001114289.2
	R: TCC CTT TCT TTT GCT TTT TCT TTA G				
CXCL10	F: ACC AAA GTG CTG TTC TTA TTT TCT G	60	262	40	DQ372065.1
	R: ATT GCT TTC AGT AAA TTC TTG ATG G				
CXCL11	F: CTT GGC TGT CAT ATT TTG TGC TAC	60	257	40	EU682377.1
	R: GGA AAT TCA TTC TTT CAA CTT TCT TC				
CXCR3	F: TGG AAA ACT CTT CCT ATG ACT ATG G	60	130	40	XM 003135179.3
	R: ACG AAG AGG AGG CTG TAG AGG				
FCGR3A	F: AGA AGG ATT CTG TGA CTC TGA AGT G	60	313	40	NM 214391.2
	R: TGG AAA TAT TGG ACC TTT TGT ATT G				
TCRA	F: CCT GAT ATC AAG AAC CCT GA	60	114	40	HM537231.1
	R: CTC CGA GTC TTT TGT TGT AT				
TCRB	F: CAA ACA CTG AAG TCT TCT TT	60	386	40	FJ944058.1
	R: CCA GTT GTA CTC CCA CTC GT				
RPL7	F: AAG CCA AGC ACT ATC ACA AGG AAT ACA	60	172	40	NM 001113217
	R: TGC AAC ACC TTT CTG ACC TTT GG				
For RT-PCR					
CXCL9	F: CAA AAA CCA AGA AAG TTC GAA AAG	60	317	35	NM 001114289.2
	R: GTA GCT AAA GCA TGA TGA AAT CCA G				
CXCL10	F: ACC AAA GTG CTG TTC TTA TTT TCT G	60	262	35	DQ372065.1
	R: ATT GCT TTC AGT AAA TTC TTG ATG G				
CXCL11	F: CTT GGC TGT CAT ATT TTG TGC TAC	60	257	35	EU682377.1
	R: GGA AAT TCA TTC TTT CAA CTT TCT TC				
CXCR3	F: TGG AAA ACT CTT CCT ATG ACT ATG G	60	130	35	XM 003135179.3
	R: ACG AAG AGG AGG CTG TAG AGG				
RPL7	F: AAG CCA AGC ACT ATC ACA AGG AAT ACA	60	172	25	NM 001113217
	R: TGC AAC ACC TTT CTG ACC TTT GG				
For in situ hybridization					
CXCL9	F: GTG ACA CTG TTC TAC CAC TAT GAA G	60	570	40	NM 001114289.2
	R: GGG ATT TTA AAA GCA ACC TTC TAG C				
CXCL10	F: ACC AAA GTG CTG TTC TTA TTT TCT G	60	734	40	DQ372065.1
	R: GAA AGC AGT AGA AGC CCA CG				

the presence of apparently normal filamentous conceptuses in uterine flushings on Days 12 and 15, and the presence of embryos and placenta on the later days of pregnancy. Uterine flushings were obtained by introducing and recovering 50 ml phosphate-buffered saline (PBS) (pH 7.4) at tissue collection (25 ml/uterine horn). Conceptus tissues on Days 12 and 15 of pregnancy were obtained from uterine flushing, and chorioallantoic tissues were obtained from Days 30, 60, 90, and 114 of pregnancy (n = 3–4/day).

Endometrium, dissected free of myometrium, was collected from the middle portion of each uterine horn, snap-frozen in liquid nitrogen, and stored at −80°C prior to RNA extraction. For in situ hybridization analysis and immunohistochemistry, cross-sections of endometrium were fixed in 4% paraformaldehyde in PBS (pH 7.4) for 24 h and then embedded in paraffin as previously described [31].

Total RNA extraction and reverse transcription-polymerase chain reaction of *CXCL9, CXCL10, CXCL11,* and *CXCR3* cDNAs

Total RNA was extracted from endometrial, chorioallantoic, conceptus tissues, and PBMC cells using TRIzol reagent (Invitrogen, Life Technology, Carlsbad, CA) according to the manufacturer's recommendation. The quantity of RNA was assessed spectrophoto-

metrically, and the integrity of RNA was validated following electrophoresis in 1% agarose gel.

Four micrograms of total RNA from endometrial, conceptus, and chorioallantoic tissues were treated with DNase I (Promega, Madison, WI) and reverse transcribed using SuperScript II Reverse Transcriptase (Invitrogen) to obtain cDNAs. The cDNA templates were then diluted 1:4 with nuclease-free water and amplified by polymerase chain reaction (PCR) using Taq polymerase (Takara Bio, Shiga, Japan). The PCR conditions and sequences of primer pairs are listed in Table 1. The PCR products were separated on a 2% agarose gel and visualized using ethidium bromide staining. The identity of each amplified PCR product was verified by sequence analysis after cloning into the pCRII vector (Invitrogen).

Quantitative real-time reverse transcription-polymerase chain reaction

To analyze expression of transcripts in the uterine endometrial and chorioallantoic tissues, real-time reverse transcription-polymerase chain reaction (RT-PCR) was performed using the Applied Biosystems StepOnePlus System (Applied Biosystems, Foster City, CA) using the SYBR Green method. The Power SYBR Green PCR Master Mix (Applied Biosystems) was used for PCR reactions. The final reaction volume of 20 μl included 2 μl of cDNA,

10 μl of 2× Master mix, 2 μl of each primer (100 nM), and 4 μl of dH$_2$O. PCR conditions and sequences of primer pairs are listed in Table 1. The intra-assay coefficient of variation for each primer set ranged from 0.30% to 0.42%. The results are reported as the expression relative to the level detected on Day 12 of the estrous cycle, the level detected on Day 30 of pregnancy, or the level detected in control explant tissues after normalization of the transcript amount to the endogenous porcine ribosomal protein L7 (*RPL7*) control by the $2^{-\Delta\Delta CT}$ method [32].

Nonradioactive in situ hybridization

The nonradioactive in situ hybridization procedure was performed as described previously [33] with minor modification. Sections (5 μm thick) were rehydrated through successive baths of xylene, 100% ethanol, 95% ethanol, diethylpyrocarbonate (DEPC)-treated water, and DEPC-treated PBS. Tissue sections were boiled in citrate buffer (pH 6.0) for 10 min. After washing in DEPC-treated PBS, they were digested using 5 μg/ml Proteinase K (Sigma, St. Louis, MO) in TE (100 mM Tris-HCl, 50 mM EDTA, pH 7.5) at 37°C. After postfixation in 4% paraformaldehyde, sections were incubated twice for 15 min each in PBS containing 0.1% active DEPC and equilibrated for 15 min in 5× saline sodium citrate (SSC). The sections were prehybridized for 2 h at 68°C in hybridization mix (50% formamide, 5× SSC, 500 μg/ml herring sperm DNA, 250 μg/ml yeast tRNA; 200 μl on each section). Sense and antisense *CXCL9* and *CXCL10* riboprobes were generated using partial cDNAs cloned into pCRII vectors by linearizing with appropriate restriction enzymes and labeling with digoxigenin (DIG)-UTP using a DIG RNA Labeling kit (Roche, Indianapolis, IN). The probes were denatured for 5 min at 80°C and added to the hybridization mix. The hybridization reaction was carried out at 68°C overnight. Prehybridization and hybridization reactions were performed in a box saturated with a 5× SSC–50% formamide solution to avoid evaporation, and no coverslips were used. After hybridization, sections were washed for 30 min in 2× SSC at room temperature, 1 h in 2× SSC at 65°C, and 1 h in 0.1× SSC at 65°C. Probes bound to the section were detected immunologically using sheep anti-DIG Fab fragments covalently coupled to alkaline phosphatase and nitroblue tetrazolium chloride/5-bromo-4-chloro-3-indolyl phosphate (toluidine salt) as chromogenic substrate, according to the manufacturer's protocol (Roche).

Immunohistochemistry

To determine the type(s) of cells expressing CXCL11 and CXCR3 in the porcine endometrium, sections were immunostained. Sections (5 μm thick) were deparaffinized and rehydrated in an alcohol gradient. Tissue sections were washed with PBS with 0.1% (v/v) Tween-20 (PBST) and blocked with 0.5% (v/v) H$_2$O$_2$ in methanol for 30 min. Tissue sections were then blocked with 10% normal goat serum for 30 min at room temperature. Rabbit polyclonal anti-CXCL11 antibody (4 μg/ml; Biorbyt, San Francisco, CA) or rabbit polyclonal anti-CD3 antibody (3 μg/ml; DAKO, Glostrup, Denmark) was added, and sections were incubated overnight at 4°C in a humidified chamber, or rabbit anti-CXCR3 antibody (10 μg/ml; LifeSpan BioSciences, Seattle, WA) was added, and sections were incubated for 3 h at room temperature. For each tissue tested, purified normal rabbit IgG was substituted for the primary antibody as a negative control. Tissue sections were washed intensively with PBST. Biotinylated goat antirabbit secondary antibody (1 μg/ml; Vector Laboratories, Burlingame, CA) was added, and sections were incubated for 1 h at room temperature. Following washes with PBST, a strep-

tavidin peroxidase conjugate (Invitrogen) was added to the tissue sections, which were then incubated for 10 min at room temperature. The sections were washed with PBST, and aminoethyl carbazole substrate (Invitrogen) was added to the tissue sections, which were then incubated for 20 min at room temperature. The tissue sections were washed in water, counterstained with Mayer's hematoxylin, and coverslipped.

For quantification of immunostained CD3$^+$ T cells, endometrial tissue sections were scanned using a TissueFAXS cytometer system (TissueGnostics, Vienna, Austria), as described previously [34]. Entire endometrial tissue sections with an average of about 150 fields per each slide were acquired using a 10× objective lens. Analysis of immunostaining signals was done using HistoQuest analysis software (TissueGnostics). The cutoff value for background staining was chosen using the forward/backward gating tool of the HistoQuest software. The HistoQuest analysis software measured mean relative intensity of CD3-positive immunostaining signals.

Explant cultures

Endometrium on Day 12 of the estrous cycle was dissected from the myometrium and placed into warm phenol red-free Dulbecco-modified Eagle medium/F-12 (DMEM/F-12) culture medium (Sigma) containing penicillin G (100 IU/ml) and streptomycin (0.1 mg/ml) as described previously [31], with some modification. The endometrium was minced with scalpel blades into small pieces (2–3 mm^3), and 500 mg was placed into T25 flasks with serum-free modified DMEM/F-12 containing 10 μg/ml insulin (Sigma), 10 ng/ml transferrin (Sigma), and 10 ng/ml hydrocortisone (Sigma). To determine the effects of IFNG on the expression of endometrial genes, endometrial explant tissues were cultured immediately after mincing in the presence of 0, 1, 10, or 100 ng/ml recombinant porcine IFNG (Sigma) with both E$_2$ (50 ng/ml) and P$_4$ (3 ng/ml) at 37°C for 24 h. Explant tissues were then harvested, and total RNA was extracted for real-time RT-PCR analysis to determine expression levels of *CXCL9*, *CXCL10*, *CXCL11*, and *CXCR3* mRNAs. These experiments were conducted using endometria from three gilts on Day 12 of the estrous cycle. Treatments were performed in triplicate using endometrial tissues obtained from each of the three gilts.

Porcine peripheral blood mononuclear cell migration assay

Whole blood obtained from approximately 6-month-old pigs was diluted with PBS at a ratio of 1:1, and PBMCs were isolated by density gradient centrifugation (400× *g* for 25 min without brake) using Ficoll-Paque Plus (Amersham Bioscience, Buckinghamshire, UK). PBMCs, suspended in RPMI 1640 medium supplemented with 10% FBS and 1% antibiotics (Invitrogen), were further used for the in vitro migration assay in response to chemokines using 0.33-cm^2 polycarbonate membrane inserts with 5.0-μm pores in 24-well tissue culture plates (Corning Inc., Corning, NY). The inserts were preincubated in RPMI 1640 containing 5% FBS for 1 h. Media were removed, and the inserts were then placed into wells containing 500 μl media containing different doses (0, 2, 5, 10, 30, or 90 ng/ml) of the recombinant porcine chemokines CXCL9 (rCXCL9), CXCL10 (rCXCL10), and CXCL11 (rCXCL11) (all from Immunochemistry Technologies, Bloomington, MN). A single-cell suspension of 1 × 10^6 PBMCs in a total volume of 200 μl media was loaded onto the inserts. Then, the plates were incubated at 37°C and in 5% CO$_2$ for 90 min, and cells that had migrated were collected and analyzed. Cells that had migrated to the lower chamber but remained

attached to the insert were recovered by initially removing the cells in the upper chamber, as well as any remaining suspension. The attached cells were then recovered by placing the bottom of the insert into 500 μl ice cold PBS containing 0.05% (w/v) trypsin-EDTA and tapping lightly. The migration index was calculated as follows: migration index = [(cell number in the lower chamber with chemokine) – (cell number in the lower chamber without chemokine)]/(the number of cells initially added).

To investigate the phenotypes of the migrated cells from PBMCs, the cells that had migrated following treatment with 10 ng/ml of chemokines were analyzed using mouse antiporcine CD3e biotin (clone PPT3; Southern Biotech, Birmingham, AL), CD4 FITC (clone 74-12-4; BD Biosciences, San Jose, CA), CD8a PE (clone 76-2-11; BD Biosciences), and CD16 biotin (clone FCG7; BD Biosciences). The biotin-conjugated antibody was detected using allophycocyanin (APC)-linked streptavidin (BioLegend, San Diego, CA) for CD3+ T cells and NK cells. The cells were incubated for 20 min at 4°C in the dark, washed, and the expression of the markers was measured using flow cytometry (FACSCantoII, BD Biosciences). All flow cytometric data were analyzed using FlowJo software (Tree Star Inc., Ashland, OR). The entire experiment was independently replicated at least three times in triplicate with different batches of PBMCs.

Statistical analysis

Data from real-time RT-PCR for *CXCL9*, *CXCL10*, *CXCL11*, *CXCR3*, *TCRA* (T cell receptor α), *TCRB* (T cell receptor β), and *FCGR3A* (Fc fragment of IgG, low affinity IIIa, receptor; CD16a)

expression and histomorphometric quantification for CD3+ T cells during the estrous cycle and pregnancy were subjected to ANOVA using the General Linear Models procedures of SAS (Cary, NC). As sources of variation, the model included day, pregnancy status (cyclic or pregnant, Days 12 and 15 postestrus), and their interactions to evaluate steady-state levels of *CXCL9*, *CXCL10*, *CXCL11*, *CXCR3*, *TCRA*, *TCRB*, and *FCGR3A* mRNAs, and CD3+ T cell numbers. Data from real-time RT-PCR performed to assess the effect of the day of pregnancy (Days 12, 15, 30, 60, 90, and 114) in the endometrium for the expression of *CXCL9*, *CXCL10*, *CXCL11*, *TCRA*, *TCRB*, and *FCGR3A* and the effect of the day of pregnancy (Days 30, 60, 90, and 114) in chorioallantoic tissue for the expression of *CXCL9*, *CXCL10*, and *CXCL11*, data from IFNG dose-response studies, and data from histomorphometry were analyzed by least squares regression analysis. Data from migration assays were analyzed by one-way ANOVA with dose of chemokines as a source of variation followed by Tukey post-test. Data are presented as mean with SEM. Differences were considered significant if $P < 0.05$.

Results

Expression of *CXCL9*, *CXCL10*, *CXCL11,* and *CXCR3* mRNAs in the endometrium during the estrous cycle and pregnancy in pigs

To determine whether *CXCL9*, *CXCL10*, *CXCL11*, and *CXCR3* mRNAs are expressed in the endometrium during the estrous cycle
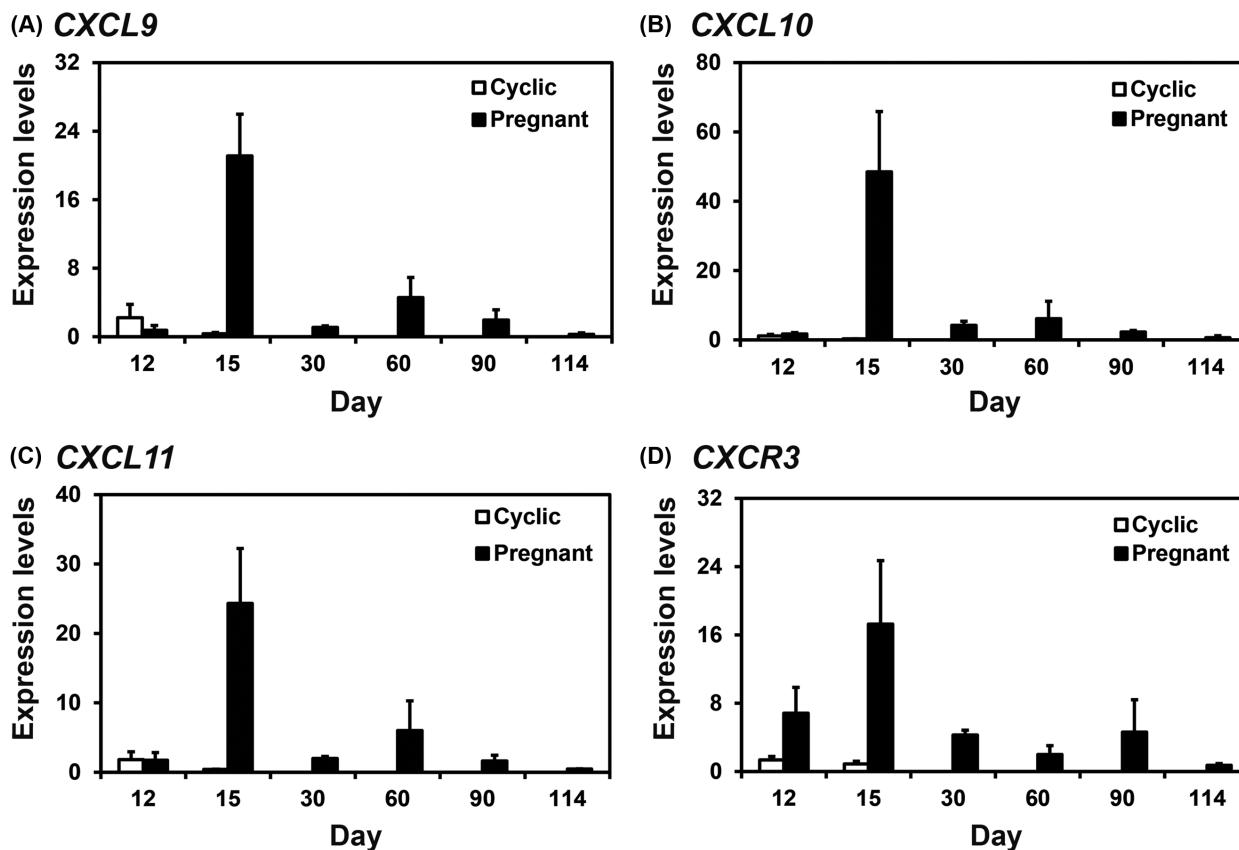
Figure 1. Expression of *CXCL9* (A), *CXCL10* (B), *CXCL11* (C), and *CXCR3* (D) mRNAs in the endometrium during the estrous cycle and pregnancy in pigs. Endometrial tissue samples from cyclic and pregnant gilts were analyzed by real-time RT-PCR, and data are reported as expression relative to that detected on Day 12 of the estrous cycle after normalization of the transcript amount to the endogenous *RPL7* control. Data are presented as mean with standard error.
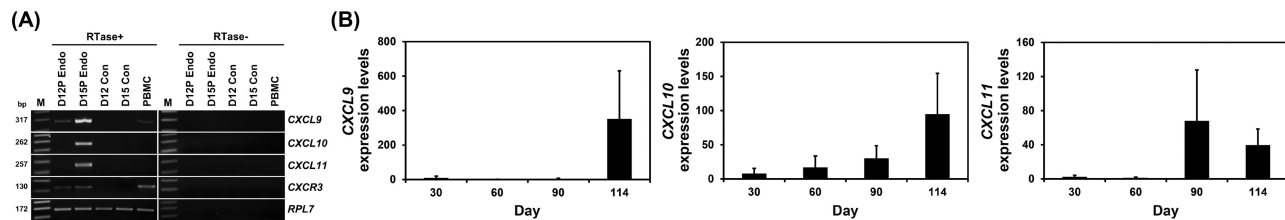
Figure 2. Expression of *CXCL9*, *CXCL10*, *CXCL11*, and *CXCR3* by conceptuses from Day 12 to Day 15 of pregnancy (A) and by chorioallantoic tissues during later stages of pregnancy (B). (A) RT-PCR analysis of *CXCL9*, *CXCL10*, *CXCL11*, and *CXCR3* mRNA in conceptuses on Day 12 and Day 15 of pregnancy was performed using total RNA preparations. *RPL7* was used as a positive control. RTase +/–, with (+) or without (–) reverse transcriptase; M, molecular marker; D12 Endo, endometrium on Day 12 of pregnancy; D12 Con, Day 12 conceptus; D15 Con, Day 15 conceptus; PBMC, peripheral blood mononuclear cells. (B) Real-time RT-PCR analysis of the expression of *CXCL9*, *CXCL10*, and *CXCL11* mRNAs in chorioallantoic tissue samples on Day 30, Day 60, Day 90, and Day 114 of pregnancy. Expression of *CXCR3* mRNA was not detectable in chorioallantoic tissues. Data are reported as expression relative to that detected on Day 30 of pregnancy after normalization of the transcript amount to the endogenous *RPL7* control, and data are presented as mean with standard error.

and pregnancy, we measured their relative abundance in the endometrium during the estrous cycle and pregnancy using real-time RT-PCR analysis. As shown in Figure 1, real-time RT-PCR analysis indicated that the abundance of *CXCL9*, *CXCL10*, *CXCL11*, and *CXCR3* mRNA was affected by day, pregnancy status, and day X status interaction on Days 12 and 15 postestrus ($P < 0.05$) and were greater on Day 15 of pregnancy than on Day 15 of the estrous cycle. During pregnancy, the abundance of *CXCL9*, *CXCL10*, *CXCL11*, and *CXCR3* mRNAs was greatest on Day 15 and was maintained at a lower abundance during the later stage of pregnancy (linear effect of day for *CXCL9*, *CXCL10*, and *CXCR3*, $P < 0.05$; quadratic effect of day for *CXCL11*, $P < 0.05$).

Expression of *CXCL9*, *CXCL10*, *CXCL11*, and *CXCR3* mRNAs in conceptuses during early pregnancy, peripheral blood mononuclear cells, and chorioallantoic tissues during later stage of pregnancy

Next, we performed RT-PCR using cDNA from conceptuses during pregnancy and porcine PBMCs and found that *CXCL9*, *CXCL10*, *CXCL11*, and *CXCR3* mRNAs were not detectable in conceptuses from either Day 12 or 15 of pregnancy (Figure 2A), whereas mRNAs for *CXCL9* and *CXCR3* were detectable in porcine PBMCs.

To determine whether the abundance of *CXCL9*, *CXCL10*, *CXCL11*, and *CXCR3* mRNAs changes in chorioallantoic tissues during pregnancy, real-time RT-PCR analysis was performed. As shown in Figure 2B, analysis of the abundance of *CXCL9*, *CXCL10*, and *CXCL11* mRNAs in chorioallantoic tissues on Days 30, 60, 90, and 114 of pregnancy revealed that abundance of *CXCL9*, *CXCL10*, and *CXCL11* increased in chorioallantoic tissues toward term pregnancy (Figure 2B). *CXCR3* mRNA was not detectable in chorioallantoic tissues during mid- to term pregnancy.

Localization of *CXCL9* and *CXCL10* mRNAs and CXCL11 and CXCR3 proteins in the endometrium during the estrous cycle and pregnancy in pigs

After analyzing the expression patterns of *CXCL9*, *CXCL10*, *CXCL11*, and *CXCR3* in the endometrium, we decided to determine the cell type(s) expressing *CXCL9*, *CXCL10*, *CXCL11*, and *CXCR3* in the endometrium. In situ hybridization analysis showed that *CXCL9* mRNA on Day 15 of pregnancy was localized mainly to vascular endothelial cells (Figure 3A), and *CXCL10* mRNA was localized exclusively to subepithelial stromal cells and endothelial cells (Figure 3B). Signals for *CXCL9* and *CXCL10* mRNA localiza-
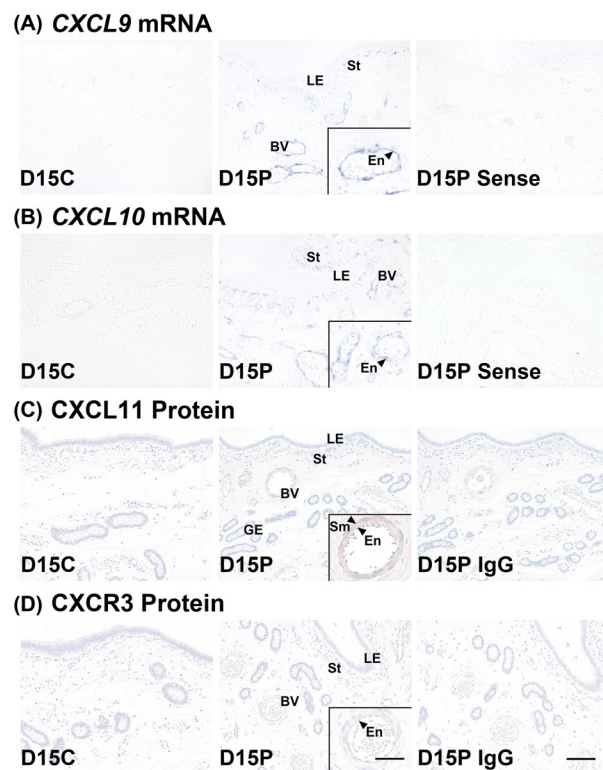
Figure 3. Localization of *CXCL9* (A) and *CXCL10* (B) mRNAs by in situ hybridization analysis and CXCL11 (C) and CXCR3 (D) proteins by immunohistochemistry in the endometrium on Day 15 of the estrous cycle and pregnancy in pigs. Representative uterine sections from Day 15 of pregnancy hybridized with DIG-labeled sense *CXCL9* or *CXCL10* cDNA probes (Sense) as a negative control for *CXCL9* and *CXCL10* are shown for in situ hybridization analysis. Representative uterine sections from Day 15 of pregnancy immunostained with normal rabbit IgG as a negative control (D15P IgG) for CXCL11 and CXCR3 are shown for immunohistochemistry analysis. D, Day; C, estrous cycle; P, pregnancy; LE, luminal epithelium; GE, glandular epithelium; St, stroma; BV, blood vessels; Sm, smooth muscle; En, endothelial cell. Scale bar = 100 μm and 50 μm in inset.

tion were rarely detectable in the endometrium during other days of pregnancy (data not shown).

Immunohistochemistry analysis demonstrated that the CXCL11 protein was localized mainly in smooth muscle cells of the blood
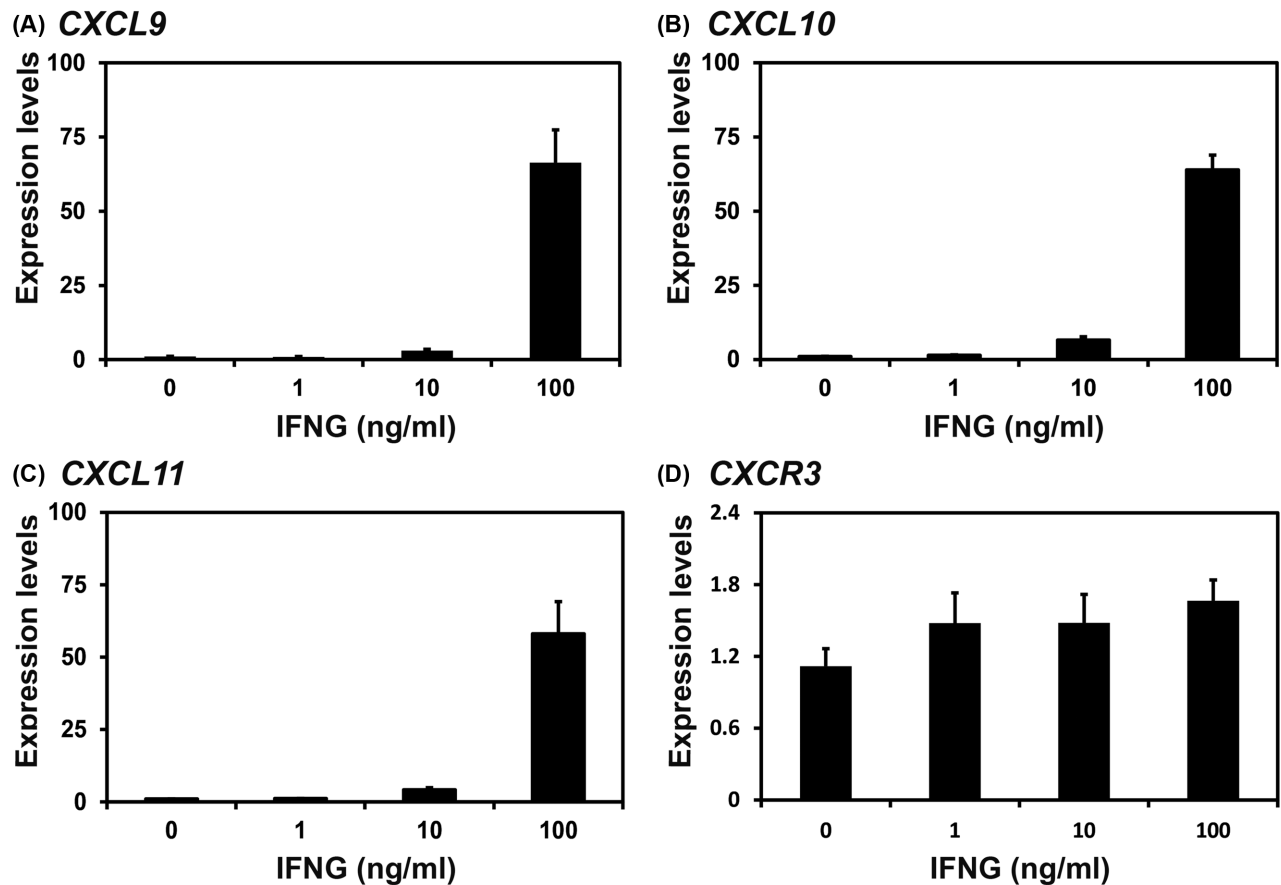
Figure 4. Effects of IFNG on *CXCL9* (A), *CXCL10* (B), *CXCL11* (C), and *CXCR3* (D) mRNA levels in endometrial explant cultures. Endometrial explants from gilts on Day 12 of the estrous cycle were cultured with 0, 1, 10, or 100 ng/ml IFNG. Abundance of mRNA expression determined by real-time RT-PCR analyses was relative to that for *CXCL9*, *CXCL10*, *CXCL11*, and *CXCR3* mRNAs in the control group (0 ng/ml IFNG) of endometrial explants after normalization of transcript amounts to *RPL7* mRNA. Data are presented as mean with standard error. These treatments were performed in triplicate using tissues obtained from each of the three gilts.

vessels on Day 15 of pregnancy (Figure 3C). CXCR3 protein was detected primarily in vascular endothelial cells on Day 15 of pregnancy, similar to that for *CXCL9* mRNA (Figure 3D). Immunohistochemistry analysis for CXCL9 and CXCL10 could not be performed due to the lack of appropriate antibodies.

### Effects of IFNG on *CXCL9, CXCL10, CXCL11*, and *CXCR3* expression in uterine endometrial tissues

Based on our results that the abundance of *CXCL9, CXCL10, CXCL11*, and *CXCR3* mRNAs in the endometrium was greatest on Day 15 of pregnancy, we next asked what factor(s) regulate *CXCL9, CXCL10, CXCL11*, and *CXCR3* expression in the endometrium. Since IFNG and IFND of conceptus origin are secreted into the uterine lumen, with the greatest abundance occurring on around Day 15 of pregnancy [1, 35], and the expression of many endometrial genes is regulated by these IFNs in pigs [11, 36], we hypothesized that IFNG may affect the expression of *CXCL9, CXCL10, CXCL11*, and *CXCR3* in the endometrium. We treated endometrial explant tissues from Day 12 of the estrous cycle with increasing doses of IFNG. As shown in Figure 3, the abundance of *CXCL9, CXCL10*, and *CXCL11* mRNAs increased in tissues treated with increasing doses of IFNG (linear effect of dose for *CXCL9, CXCL10*, and

CXCL11, $P < 0.01$), but the abundance of *CXCR3* mRNAs was not affected by IFNG.

Effects of CXCL9, CXCL10, and CXCL11 on migration of peripheral blood mononuclear cells

As the abundance of the *CXCL9, CXCL10*, and *CXCL11* mRNAs in the endometrium during pregnancy was greatest on Day 15 (Figures 1, 3, and 4), and because it is known that the CXCL9, CXCL10, and CXCL11 proteins are chemoattractant cytokines [17], and that expression of *CXCR3* mRNA is detectable in porcine PBMCs (Figure 2A), we hypothesized that CXCL9, CXCL10, and CXCL11 may affect immune cell recruitment into the endometrium during early pregnancy. Thus, we analyzed the chemotactic effect of the CXCL9, CXCL10, and CXCL11 proteins on the migration of PBMCs. As shown in Figure 5, treatment with rCXCL9 at 10 ng/ml or greater doses and rCXCL10 and rCXCL11 at 2 ng/ml or greater doses significantly increased migration of PBMCs compared to the control ($P < 0.05$).

Next, to verify whether the infiltration of T cells and NK cells into the endometrium during early pregnancy was indeed affected by these chemokines, we analyzed the effects of rCXCL9, rCXCL10, and rCXCL11 on the migration of CD4^{+}, CD8^{+}, and CD4^{+}CD8^{+}
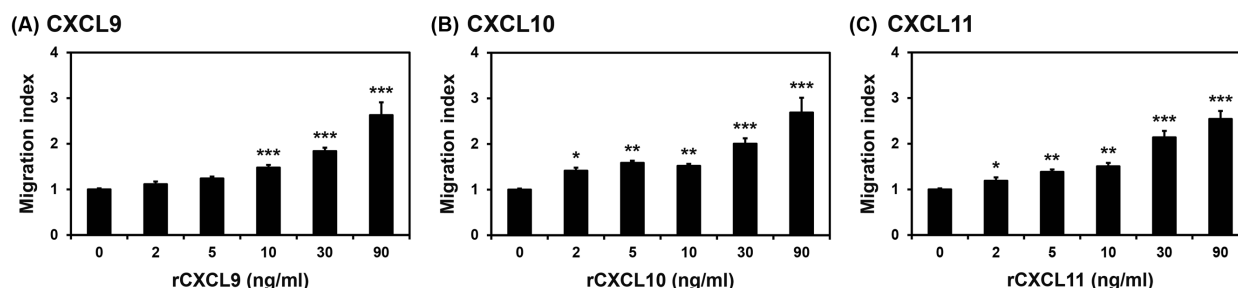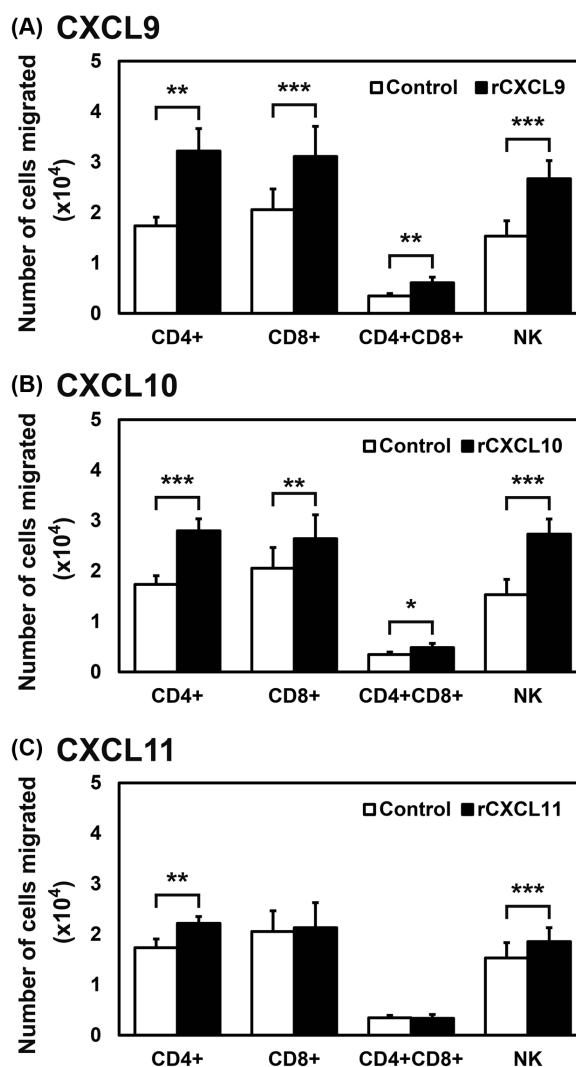
Figure 5. Effects of CXCL9 (A), CXCL10 (B), and CXCL11 (C) on migration of PBMCs. Peripheral blood mononuclear cells (PBMCs) were loaded onto an insert placed into a well of a $5.0\text{-}\mu$m-pore transwell plate containing complete media with chemokines (0, 2, 5, 10, 30, or 90 ng/ml of rCXCL9, rCXCL10, or rCXCL11). The plate then was incubated at 37°C and 5% CO_2 for 90 min, and the total number of cells that had migrated was counted. The experiment was replicated at least three times in triplicate, with different batches of PBMCs from different gilts. Data are presented as mean with standard error.

T cells and NK cells among PBMCs. As shown in Figure 6, treatment with rCXCL9, rCXCL10, and rCXCL11 significantly increased the number of migrated $CD4^+$ T cells ($P < 0.01$ for rCXCL9 and rCXCL11; $P < 0.01$ for rCXCL10) and NK cells ($P < 0.001$ for rCXCL9, rCXCL10, and rCXCL11). In addition, rCXCL9, rCXCL10, but not rCXCL11, significantly increased the number of migrated $CD8^+$ ($P < 0.001$ for rCXCL9; $P < 0.01$ for rCXCL10) and $CD4^+CD8^+$ T cells ($P < 0.01$ for rCXCL9; $P < 0.05$ for rCXCL10) compared to the control.

Expression of *TCRA*, *TCRB*, and *FCGR3A* mRNAs and immunohistochemical analysis of $CD3^+$ T cells in the endometrium during the estrous cycle and pregnancy in pigs

Having determined that CXCL9, CXCL10, and CXCL11 proteins increased the migration of T cells and NK cells, we next asked if the infiltration of T cells and NK cells into the endometrium increases at the time of endometrial CXCL9, CXCL10, and CXCL11 induction. Thus, we analyzed the expression of T cell receptor α and β chains *TCRA* and *TCRB* and an NK cell marker *FCGR3A* in the endometrium during the estrous cycle and pregnancy using real-time RT-PCR analysis. As shown in Figure 7A-C, the abundance of *TCRA*, *TCRB*, and *FCGR3A* mRNAs was affected by day, pregnancy status, and day X status interaction on Days 12 and 15 postestrus ($P < 0.01$) and was greater on Day 15 of pregnancy than on Day 15 of the estrous cycle. During pregnancy, the abundance of *TCRA*, *TCRB*, and *FCGR3A* mRNAs was greatest on Day 15 and decreased thereafter (linear effect of day for *TCRA* and *TCRB*, but not for *FCGR3A*, $P < 0.05$).

Furthermore, we localized $CD3^+$ T cells by immunohistochemistry and measured the number of $CD3^+$ T cells by histomorphometry in the endometrium during the estrous cycle and pregnancy. As shown in Figure 7D, $CD3^+$ T cells were detected in the endometrium with the increased number of endometrial $CD3^+$ T cells on Day 15 of pregnancy. $CD3^+$ T cells were also detected in adult spleen that was used as a positive control tissue. Histomorphometric analysis showed that the number of $CD3^+$ T cells in the endometrium was affected by day, pregnancy status, and day X status interaction on Days 12 and 15 postestrus ($P < 0.05$) and greater on Day 15 of pregnancy than on Day 15 of the estrous cycle. During pregnancy, the number of $CD3^+$ T cells was greatest on Day 15 and decreased thereafter (linear effect of day, $P < 0.01$) (Figure 7E).

Figure 6. Effects of CXCL9 (A), CXCL10 (B), and CXCL11 (C) on migration of $CD4^+$, $CD8^+$, $CD4^+CD8^+$ T cells, and NK cells. Peripheral blood mononuclear cells (PBMCs) were loaded onto an insert placed into a well containing 500 ml of complete media alone or media containing 10 ng/ml of rCXCL9, rCXCL10, or rCXCL11. Migrated cells were examined by staining with mouse antiporcine CD3, CD4, CD8a, and CD16 antibodies. $CD3^+$ T cells and NK cells ($CD3^-CD8a^+CD16^+$) were analyzed by flow cytometry. The experiment was replicated at least three times in triplicate with different batches of PBMCs from different gilts. Data are presented as mean with standard error.
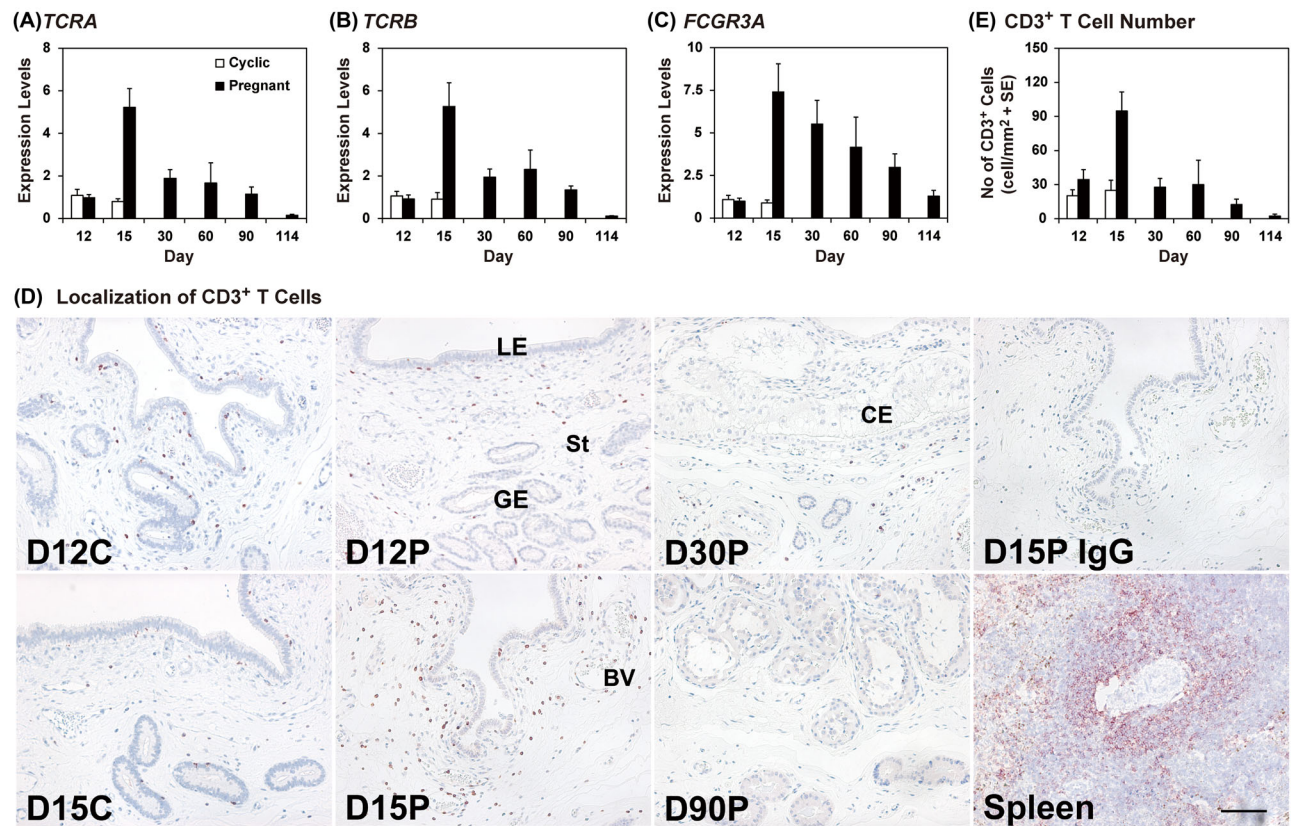
Figure 7. Expression of *TCRA* (A), *TCRB* (B), and *FCGR3A* (C) mRNAs and analysis of CD3$^+$ T cells by immunohistochemistry (D) and histomorphometry (E) in the endometrium during the estrous cycle and pregnancy in pigs. (A–C) Endometrial tissue samples from cyclic and pregnant gilts were analyzed by real-time RT-PCR, and data are reported as expression relative to that detected on Day 12 of the estrous cycle after normalization of the transcript amount to the endogenous *RPL7* control. Data are presented as mean with standard error. (D) Localization of CD3$^+$ T cells by immunohistochemistry in the endometrium. A tissue section from adult spleen stained with anti-CD3 antibody is shown as a positive control, and a tissue section from endometrium on Day 15 of pregnancy stained with normal rabbit IgG served as a negative control (D15P IgG). D, Day; C, estrous cycle; P, pregnancy; LE, luminal epithelium; GE, glandular epithelium; St, stroma; BV, blood vessels; CE, chorionic epithelium. Scale bar = 100 μm. (E) Histomorphometric quantification of CD3$^+$ T cells in the endometrium. Immunostaining signals for CD3$^+$ T cells throughout endometrial tissues was assessed by scanning using a TissueFAXS cytometer and analyzed by HistoQuest software. The software measured mean signal intensity, and data are presented as mean with standard error.

Discussion

The significant findings of the present study are as follows: (1) *CXCL9*, *CXCL10*, *CXCL11*, and their receptor *CXCR3* are expressed in the endometrium in a pregnancy status and stage-dependent manner during pregnancy; (2) *CXCL9*, *CXCL10*, *CXCL11*, and *CXCR3* mRNAs are not detectable in early-stage conceptuses, while *CXCL9*, *CXCL10*, *CXCL11*, but not *CXCR3*, mRNAs are expressed in chorioallantoic tissues during late pregnancy; (3) endometrial expression of *CXCL9*, *CXCL10*, *CXCL11*, and *CXCR3* is cell-type-specific; (4) IFNG increases the expression of *CXCL9*, *CXCL10*, *CXCL11*, but not *CXCR3*, mRNAs in endometrial tissues; (5) rCXCL9, rCXCL10, and rCXCL11 induce migration of CD4$^+$, CD8$^+$, CD4$^+$CD8$^+$ T cells, and/or NK cells, and (6) the expression of *TCRA*, *TCRB*, and *FCGR3A* mRNAs and the number of CD3$^+$ T cells in the endometrium were greatest on Day 15 of pregnancy. To the best of our knowledge, this is the first report characterizing the expression profiles of CXCL9, CXCL10, and CXCL11 and their roles at the maternal–conceptus interface during pregnancy in pigs.

The expression of CXCL9, CXCL10, and CXCL11, and their receptor CXCR3 at the maternal–conceptus interface has been demon-

strated in humans, sheep, and goats [24–26, 28]. In pigs, we found that *CXCL9*, *CXCL10*, *CXCL11*, and *CXCR3* mRNAs were also expressed in the endometrium with unique expression patterns during pregnancy. Especially, the abundance of *CXCL9*, *CXCL10*, *CXCL11*, and *CXCR3* mRNAs were greatest on Day 15 of pregnancy and decreased thereafter, making us to hypothesize that these chemokines are involved in recruitment of immune cells into the endometrium during the implantation period. The finding of great abundance of *CXCL9*, *CXCL10*, and *CXCL11*, and their receptor during early pregnancy in pigs is similar to the result shown in sheep and goat, in which the expression of these chemokines is abundant at the time of implantation [27, 28], although mRNA expression was not monitored throughout the whole gestation period in those species.

The implanting conceptuses secrete a great amount of IFNs (i.e., IFND and IFNG) between Days 14 and 16 of pregnancy in pigs; in ruminants, a great amount of IFNT are secreted between Days 13 and 21 of pregnancy [1]. It has been shown that IFNs induce *CXCL9*, *CXCL10*, and *CXCL11* mRNAs in many tissues [20]. Since our study showed that the abundance of *CXCL9*, *CXCL10*, *CXCL11*, and *CXCR3* mRNAs were greatest on Day 15 of

pregnancy, coincident with a great amount of IFND and IFNG secretion by conceptuses, we hypothesized that these IFNs might increase the endometrial expression of *CXCL9*, *CXCL10*, *CXCL11*, and *CXCR3* mRNAs. Indeed, IFNG increased the expression of *CXCL9*, *CXCL10*, and *CXCL11*, but not *CXCR3*, mRNAs in endometrial explant tissue cultures in the present study. In sheep, it has been shown that IFNT induces *CXCL10* expression in endometrial monocytes [27]. Collectively, IFNG of conceptus origin may induce the expression of *CXCL9*, *CXCL10*, and *CXCL11* mRNAs in the endometrium during the implantation period in pigs. Furthermore, conceptus-derived IFNs may be responsible for the induction of endometrial *CXCL9*, *CXCL10*, and *CXCL11* expression during the implantation period in pigs and sheep. The effect of IFND on endometrial *CXCL9*, *CXCL10*, and *CXCL11* expression, together with a regulatory mechanism for endometrial *CXCR3* expression, has yet to be further defined.

In the human endometrium, it has been shown that the expression of CXCL9, CXCL10, and CXCL11 is localized to endometrial epithelial cells and stromal cells [24, 25]. In sheep, CXCL10 expression is localized to endometrial stromal cells, most likely immune cells [27]. In the present study of pigs, *CXCL9* mRNA was predominantly localized to endothelial cells of blood vessels, while *CXCL10* mRNA localized in subepithelial stromal and endothelial cells of blood vessels, but not in epithelial cells. In addition, CXCL11 protein was mainly detected in the smooth muscle cells of blood vessels. These results indicate that *CXCL9*, *CXCL10*, and *CXCL11* in the endometrium are expressed in a species-specific and cell-type-dependent manner. *CXCR3* expression has been shown mainly on immune cells, including T cells, dendritic cells, monocytes, and NK cells, and some other cell types, such as endothelial cells and neurons [19]. CXCR3 expression in the human endometrium has been demonstrated in epithelial cells, stromal cells, and uterine NK cells [25, 26]. In the present study, CXCR3 protein was localized to vascular endothelial cells in the endometrium. In addition, *CXCR3* mRNA was abundantly expressed in PBMCs. Localization of CXCL9, CXCL10, CXCL11, and their receptor CXCR3 in the porcine endometrium during early pregnancy suggests that these chemokines may act not only on vascular endothelial cells in an autocrine and/or paracrine manner, but also on PBMCs.

Expression of chemokines and their receptors in the implanting conceptus has been demonstrated in several species. In humans, CXCL12 is expressed in invading trophoblasts to recruit uterine NK cells into decidua, and CXCL16 induces invasiveness and growth of trophoblasts [37–39]. In addition, CX3CL1, CCL7, and their receptors are expressed in the placenta to promote migration and invasion of trophoblasts in humans [40]. Ectoplacental cone trophoblasts in mice express CCR3, CCR5, and CXCR4, while CXCL14 expressed by trophoblast inhibits trophoblast outgrowth [41]. In pigs, *CCL4* and its receptor *ACKR2* (atypical chemokine receptor 2) are expressed in the early-stage conceptus, although their function at the maternal–conceptus interface is not well understood [42, 43]. Our recent study demonstrated that porcine conceptuses express CCR10, a receptor for CCL28 expressed in the endometrium and conceptus [44]. Moreover, CCL28 induces proliferation and migration of porcine trophectoderm cells by activating the CCR10 signaling pathway. In sheep and goats, CXCR3 is expressed in conceptuses during the implantation period, CXCL9 and CXCL10 increase adhesion of ovine trophectoderm cells to extracellular matrix proteins, and CXCL10 increases the migration of caprine trophoblast cells [28, 29]. However, in the present study in pigs, we found that expression

of *CXCL9*, *CXCL10*, *CXCL11*, and *CXCR3* mRNAs was rarely detectable in the conceptus during early pregnancy. It is probable that chemokines involved in proliferation, migration, and adhesion of trophectoderm cells during the initial stage of implantation are different between pigs and ruminants, even though these species form a similar epitheliochorial type of placenta. Interestingly, we observed that chorioallantoic tissues during late pregnancy in pigs expressed *CXCL9*, *CXCL10*, and *CXCL11* mRNAs, but not *CXCR3* mRNAs. However, the roles of CXCL9, CXCL10, and CXCL11 derived from chorioallantoic tissues during late pregnancy still need to be investigated.

Given that the primary role of chemokines is chemotaxis [19], and that CXCR3 is expressed in PBMCs, we hypothesized that CXCL9, CXCL10, and CXCL11 produced by endometrial cells may act on recruitment of immune cells from circulating blood into the endometrial tissues. Indeed, CXCL9, CXCL10, and CXCL11 increased migration of PBMCs, suggesting that these cytokines may act on recruitment of immune cells into the endometrium. To further understand which types of cells among PBMCs are recruited, we analyzed the numbers of CD4+ T cells, CD8+ T cells, CD4+CD8+ T cells, and NK cells that migrated when exposed to CXCL9, CXCL10, and CXCL11. T cells and NK cells are the major cell types expressing CXCR3 among immune cells [19], and these cell types are known to play important roles at the maternal–conceptus interface during pregnancy [45, 46]. Interestingly, migration of CD4+ T cells and NK cells was increased by rCXCL9, rCXCL10, and rCXCL11, while migration of CD8+ and CD4+CD8+ T cells was increased by rCXCL9, rCXCL10, but not rCXCL11, suggesting different biological activities of CXCL9, CXCL10, and CXCL11 on the migration of immune cells. It has been reported that CD4+ T cells, CD8+ T cells, and NK cells are present in the porcine endometrium during early pregnancy [45–48]. In this study, we also analyzed the expression of *TCRA*, *TCRB*, *FCGR3A* mRNAs and the number of CD3+ T cells in the endometrium to determine the infiltration of T cells and NK cells into the endometrium at the time of endometrial CXCL9, CXCL10, and CXCL11 induction. Our data showed that the abundance of T cell receptor subunits *TCRA* and *TCRB* expression, the number of CD3+ T cells in the endometrium, and the abundance of an NK cell surface marker *FCGR3A* (CD16) expression were greatest on Day 15 of pregnancy and decreased thereafter throughout gestation. Thus, these data suggest that T cells and NK cells in the endometrium during early pregnancy are recruited, at least in part, by CXCL9, CXCL10, and/or CXCL11 produced by endometrial cells in response to IFNG of conceptus origin. However, further investigation will be required to obtain in vivo evidence for these and any other factor(s), if any, of their involvement in T and NK cell recruitment into the endometrium at the time of implantation.

Although we did not further investigate the effects of CXCL9, CXCL10, and CXCL11 on endothelial cells, which express CXCR3, it has been shown that they mediate angiostatic activity by inhibiting proliferation and tube formation of endothelial cells at the late stage of the wound healing process and activate dissociation of newly formed blood vessels [49–51]. In addition, CXCL10 induces transendothelial migration of T cell in the presence of endothelial cells [52], and regulatory T cell recruitment to the endothelial cells is promoted by the presence of CXCR3 [53]. These findings suggest the possibility that CXCL9, CXCL10, and CXCL11 may act on endothelial cells expressing CXCR3 to regulate endothelial proliferation and the integrity of blood vessels and activate the infiltration of immune cells into the endometrium at the time of implantation in pigs.

In conclusion, our results indicate that the chemokine ligands CXCL9, CXCL10, and CXCL11 and their receptor, CXCR3, are expressed in the endometrium in a pregnancy stage-dependent and cell type-specific manner, with the greatest abundance being expressed on Day 15 of pregnancy. IFNG of conceptus origin induces endometrial expression of CXCL9, CXCL10, and CXCL11, which, in turn, may act on the recruitment of CD4^{+}, CD8^{+}, CD4^{+}CD8^{+} T cells, and NK cells into the endometrium during early pregnancy. These results provide important insights into the regulation of maternal immune responses to IFNG from the developing conceptus at the maternal–fetal interface in pigs, which form a true epitheliochorial placenta.

Acknowledgment

References

1. Bazer FW, Johnson GA. Pig blastocyst-uterine interactions. *Differentiation* 2014; **87**:52–65.
2. Mathew DJ, Newsom EM, Guyton JM, Tuggle CK, Geisert RD, Lucy MC. Activation of the transcription factor nuclear factor-kappa B in uterine luminal epithelial cells by interleukin 1 Beta 2: a novel interleukin 1 expressed by the elongating pig conceptus. *Biol Reprod* 2015; **92**:107.
3. Seo H, Choi Y, Shim J, Choi Y, Ka H. Regulatory mechanism for expression of IL1B receptors in the uterine endometrium and effects of IL1B on prostaglandin synthetic enzymes during the implantation period in pigs. *Biol Reprod* 2012; **87**:31.
4. Seo H, Choi Y, Shim J, Yoo I, Ka H. Comprehensive analysis of prostaglandin metabolic enzyme expression during pregnancy and the characterization of AKR1B1 as a prostaglandin F synthase at the maternal-conceptus interface in pigs. *Biol Reprod* 2014; **90**:99.
5. Seo H, Choi Y, Shim J, Yoo I, Ka H. Prostaglandin transporters ABCC4 and SLCO2A1 in the uterine endometrium and conceptus during pregnancy in pigs. *Biol Reprod* 2014; **90**:100.
6. Cencic A, Guillomot M, Koren S, La Bonnardiere C. Trophoblastic interferons: do they modulate uterine cellular markers at the time of conceptus attachment in the pig? *Placenta* 2003; **24**:862–869.
7. Platanias LC. Mechanisms of type-I- and type-II-interferon-mediated signaling. *Nat Rev Immunol* 2005; **5**:375–386.
8. Bazer FW, Burghardt RC, Johnson GA, Spencer TE, Wu G. Interferons and progesterone for establishment and maintenance of pregnancy: interactions among novel cell signaling pathways. *Reprod Biol* 2008; **8**:179–211.
9. Lefevre F, Martinat-Botte F, Locatelli A, De Niu P, Terqui M, La Bonnardiere C. Intrauterine infusion of high doses of pig trophoblast interferons has no antiluteolytic effect in cyclic gilts. *Biol Reprod* 1998; **58**:1026–1031.
10. Murphy SP, Tayade C, Ashkar AA, Hatta K, Zhang J, Croy BA. Interferon gamma in successful pregnancies. *Biol Reprod* 2009; **80**:848–859.
11. Joyce MM, Burghardt JR, Burghardt RC, Hooper RN, Jaeger LA, Spencer TE, Bazer FW, Johnson GA. Pig conceptuses increase uterine interferon-regulatory factor 1 (IRF1), but restrict expression to stroma through estrogen-induced IRF2 in luminal epithelium. *Biol Reprod* 2007; **77**:292–302.
12. Joyce MM, Burghardt JR, Burghardt RC, Hooper RN, Bazer FW, Johnson GA. Uterine MHC class I molecules and beta 2-microglobulin are regulated by progesterone and conceptus interferons during pig pregnancy. *J Immunol* 2008; **181**:2494–2505.
13. Butcher EC, Picker LJ. Lymphocyte homing and homeostasis. *Science* 1996; **272**:60–66.
14. Olson TS, Ley K. Chemokines and chemokine receptors in leukocyte trafficking. *Am J Physiol Regul Integr Comp Physiol* 2002; **283**:R7–R28.
15. Gasperini S, Marchi M, Calzetti F, Laudanna C, Vicentini L, Olsen H, Murphy M, Liao F, Farber J, Cassatella MA. Gene expression and production of the monokine induced by IFN-gamma (MIG), IFN-inducible T cell alpha chemoattractant (I-TAC), and IFN-gamma-inducible protein-10 (IP-10) chemokines by human neutrophils. *J Immunol* 1999; **162**:4928–4937.
16. Cole KE, Strick CA, Paradis TJ, Ogborne KT, Loetscher M, Gladue RP, Lin W, Boyd JG, Moser B, Wood DE, Sahagan BG, Neote K. Interferon-inducible T cell alpha chemoattractant (I-TAC): a novel non-ELR CXC chemokine with potent activity on activated T cells through selective high affinity binding to CXCR3. *J Exp Med* 1998; **187**:2009–2021.
17. Farber JM. Mig and IP-10: CXC chemokines that target lymphocytes. *J Leukoc Biol* 1997; **61**:246–257.
18. Proost P, Verpoest S, Van de Borne K, Schutyser E, Struyf S, Put W, Ronsse I, Grillet B, Opdenakker G, Van Damme J. Synergistic induction of CXCL9 and CXCL11 by Toll-like receptor ligands and interferon-gamma in fibroblasts correlates with elevated levels of CXCR3 ligands in septic arthritis synovial fluids. *J Leukoc Biol* 2004; **75**:777–784.
19. Liu L, Callahan MK, Huang D, Ransohoff RM. Chemokine receptor CXCR3: an unexpected enigma. *Curr Top Dev Biol* 2005; **68**:149–181.
20. Groom JR, Luster AD. CXCR3 ligands: redundant, collaborative and antagonistic functions. *Immunol Cell Biol* 2011; **89**:207–215.
21. Inngjerdingen M, Damaj B, Maghazachi AA. Expression and regulation of chemokine receptors in human natural killer cells. *Blood* 2001; **97**:367–375.
22. Jinquan T, Jing C, Jacobi HH, Reimert CM, Millner A, Quan S, Hansen JB, Dissing S, Malling HJ, Skov PS, Poulsen LK. CXCR3 expression and activation of eosinophils: role of IFN-gamma-inducible protein-10 and monokine induced by IFN-gamma. *J Immunol* 2000; **165**:1548–1556.
23. Cella M, Jarrossay D, Facchetti F, Alebardi O, Nakajima H, Lanzavecchia A, Colonna M. Plasmacytoid monocytes migrate to inflamed lymph nodes and produce large amounts of type I interferon. *Nat Med* 1999; **5**:919–923.
24. Kitaya K, Nakayama T, Daikoku N, Fushiki S, Honjo H. Spatial and temporal expression of ligands for CXCR3 and CXCR4 in human endometrium. *J Clin Endocrinol Metab* 2004; **89**:2470–2476.
25. Hirota Y, Osuga Y, Koga K, Yoshino O, Hirata T, Morimoto C, Harada M, Takemura Y, Nose E, Yano T, Tsutsumi O, Taketani Y. The expression and possible roles of chemokine CXCL11 and its receptor CXCR3 in the human endometrium. *J Immunol* 2006; **177**:8813–8821.
26. Sentman CL, Meadows SK, Wira CR, Eriksson M. Recruitment of uterine NK cells: induction of CXC chemokine ligands 10 and 11 in human endometrium by estradiol and progesterone. *J Immunol* 2004; **173**:6760–6766.
27. Nagaoka K, Sakai A, Nojima H, Suda Y, Yokomizo Y, Imakawa K, Sakai S, Christenson RK. A chemokine, interferon (IFN)-gamma-inducible protein 10 kDa, is stimulated by IFN-tau and recruits immune cells in the ovine endometrium. *Biol Reprod* 2003; **68**:1413–1421.
28. Imakawa K, Imai M, Sakai A, Suzuki M, Nagaoka K, Sakai S, Lee SR, Chang KT, Echternkamp SE, Christenson RK. Regulation of conceptus adhesion by endometrial CXC chemokines during the implantation period in sheep. *Mol Reprod Dev* 2006; **73**:850–858.
29. Nagaoka K, Nojima H, Watanabe F, Chang KT, Christenson RK, Sakai S, Imakawa K. Regulation of blastocyst migration, apposition, and initial adhesion by a chemokine, interferon gamma-inducible protein 10 kDa (IP-10), during early gestation. *J Biol Chem* 2003; **278**:29048–29056.
30. Imakawa K, Nagaoka K, Nojima H, Hara Y, Christenson RK. Changes in immune cell distribution and IL-10 production are regulated through endometrial IP-10 expression in the goat uterus. *Am J Reprod Immunol* 2005; **53**:54–64.
31. Seo H, Kim M, Choi Y, Lee CK, Ka H. Analysis of lysophosphatidic acid (LPA) receptor and LPA-induced endometrial prostaglandin-endoperoxide synthase 2 expression in the porcine uterus. *Endocrinology* 2008; **149**:6166–6175.
32. Livak KJ, Schmittgen TD. Analysis of relative gene expression data using real-time quantitative PCR and the 2(-Delta Delta C(T)) Method. *Methods* 2001; **25**:402–408.

33. Braissant O, Wahli W. A simplified in situ hybridization protocol using non-radioactively labeled probes to detect abundant and rare mRNAs on tissue sections. *Biochemica* 1998; **1**:10–16.

34. Kim M, Seo H, Choi Y, Shim J, Bazer FW, Ka H. Swine leukocyte antigen-DQ expression and its regulation by interferon-gamma at the maternal-fetal interface in pigs. *Biol Reprod* 2012; **86**:43

35. La Bonnardiere C, Martinat-Botte F, Terqui M, Lefevre F, Zouari K, Martal J, Bazer F. Production of two species of interferon by Large White and Meishan pig conceptuses during the peri-attachment period. *J Reprod Fertil* 1991; **91**:469–478.

36. Johnson GA, Bazer FW, Burghardt RC, Spencer TE, Wu G, Bayless KJ. Conceptus-uterus interactions in pigs: endometrial gene expression in response to estrogens and interferons from conceptuses. *Soc Reprod Fertil Suppl* 2009; **66**:321–332.

37. Huang Y, Zhu XY, Du MR, Wu X, Wang MY, Li DJ. Chemokine CXCL16, a scavenger receptor, induces proliferation and invasion of first-trimester human trophoblast cells in an autocrine manner. *Hum Reprod* 2006; **21**:1083–1091.

38. Dimitriadis E, Nie G, Hannan NJ, Paiva P, Salamonsen LA. Local regulation of implantation at the human fetal-maternal interface. *Int J Dev Biol* 2010; **54**:313–322.

39. Arck PC, Hecher K. Fetomaternal immune cross-talk and its consequences for maternal and offspring's health. *Nature Med* 2013; **99**:548–556.

40. Hannan NJ, Jones RL, White CA, Salamonsen LA. The chemokines, CX3CL1, CCL14, and CCL4, promote human trophoblast migration at the feto-maternal interface. *Biol Reprod* 2006; **74**:896–904.

41. Kuang H, Chen Q, Fan X, Zhang Y, Zhang L, Peng H, Cao Y, Duan E. CXCL14 inhibits trophoblast outgrowth via a paracrine/autocrine manner during early pregnancy in mice. *J Cell Physiol* 2009; **221**:448–457.

42. Croy BA, Wessels J, Linton N, Tayade C. Comparison of immune cell recruitment and function in endometrium during development of epitheliochorial (pig) and hemochorial (mouse and human) placentas. *Placenta* 2009; **30**(suppl A):S26–S31.

43. Wessels JM, Linton NF, van den Heuvel MJ, Cnossen SA, Edwards AK, Croy BA, Tayade C. Expression of chemokine decoy receptors and their ligands at the porcine maternal-fetal interface. *Immunol Cell Biol* 2011; **89**:304–313.

44. Choi Y, Seo H, Han J, Yoo I, Kim J, Ka H. Chemokine (C-C motif) ligand 28 and its receptor CCR10: expression and function at the maternal-conceptus interface in pigs. *Biol Reprod* 2016; **95**:84.

45. Croy BA, van den Heuvel MJ, Borzychowski AM, Tayade C. Uterine natural killer cells: a specialized differentiation regulated by ovarian hormones. *Immunol Rev* 2006; **214**:161–185.

46. Engelhardt H, Croy BA, King GJ. Evaluation of natural killer cell recruitment to embryonic attachment sites during early porcine pregnancy. *Biol Reprod* 2002; **66**:1185–1192.

47. Mjosberg J, Berg G, Jenmalm MC, Ernerudh J. FOXP3+ regulatory T cells and T helper 1, T helper 2, and T helper 17 cells in human early pregnancy decidua. *Biol Reprod* 2010; **82**:698–705.

48. Kaeoket K, Persson E, Dalin AM. Influence of pre-ovulatory insemination and early pregnancy on the distribution of CD2, CD4, CD8 and MHC class II expressing cells in the sow endometrium. *Anim Reprod Sci* 2003; **76**:231–244.

49. Romagnani P, Annunziato F, Lasagni L, Lazzeri E, Beltrame C, Francalanci M, Uguccioni M, Galli G, Cosmi L, Maurenzig L, Baggiolini M, Maggi E et al. Cell cycle-dependent expression of CXC chemokine receptor 3 by endothelial cells mediates angiostatic activity. *J Clin Invest* 2001; **107**:53–63.

50. Bodnar RJ, Yates CC, Wells A. IP-10 blocks vascular endothelial growth factor-induced endothelial cell motility and tube formation via inhibition of calpain. *Circ Res* 2006; **98**:617–625.

51. Huen AC, Wells A. The beginning of the end: CXCR3 signaling in late-stage wound healing. *Adv Wound Care* 2012; **1**:244–248.

52. Newton P, O'Boyle G, Jenkins Y, Ali S, Kirby JA. T cell extravasation: demonstration of synergy between activation of CXCR3 and the T cell receptor. *Mol Immunol* 2009; **47**:485–492.

53. Ehirchiou D, Muller YD, Chicheportiche R, Nobari RH, Madelon N, Schneider MK, Seebach JD. Chemoattractant signals and adhesion molecules promoting human regulatory T cell recruitment to porcine endothelium. *Transplantation* 2016; **100**:753–762.